Contrast Reversal in Scanning Tunneling Microscopy and Its Implications for the Topological Classification of SmB$_6$

Hannes Herrmann, Peter Hlawenka, Konrad Siemensmeyer, Eugen Weschke, Jaime Sánchez-Barriga, Andrei Varykhalov, Natalya Y. Shitsevalova, Anatoliy V. Dukhnenko, Volodymyr B. Filipov, Slavomir Gabáni, Karol Flachbart, Oliver Rader, Martin Sterrer, and Emile D. L. Rienks*

SmB$_6$ has recently attracted considerable interest as a candidate for the first strongly correlated topological insulator. Such materials promise entirely new properties such as correlation-enhanced bulk bandgaps or a Fermi surface from spin excitations. Whether SmB$_6$ and its surface states are topological or trivial is still heavily disputed however, and a solution is hindered by major disagreement between angle-resolved photoemission (ARPES) and scanning tunneling microscopy (STM) results. Here, a combined ARPES and STM experiment is conducted. It is discovered that the STM contrast strongly depends on the bias voltage and reverses its sign beyond 1 V. It is shown that the understanding of this contrast reversal is the clue to resolving the discrepancy between ARPES and STM results. In particular, the scanning tunneling spectra reflect a low-energy electronic structure at the surface, which supports a trivial origin of the surface states and the surface metallicity of SmB$_6$.

Since topological insulators were established, a lot of interest has turned to systems combining nontrivial topology with stronger electron correlation. The electron correlation will help to suppress the bulk conductivity which is an issue with the weakly correlated topological band insulators known to date.[1] Strongly correlated topological insulators also hold the promise of novel phenomena such as spin-charge separated excitations that form a Fermi surface.[2] Dzero et al. opened an important avenue to correlated topological insulators, by pointing out that

Kondo insulators mix local and itinerant states of opposite parity.[3]

SmB$_6$ is known historically as the first mixed valent compound and Kondo insulator and the proposal that it could be the first topological Kondo insulator reinvigorated interest in this material.[4] Early results seemingly confirmed the idea: Only the surface was found to remain conductive at low temperature,[5,6] and surface states were found at the $\overline{\Gamma}$ and $\overline{X}$ points of the surface Brillouin zone conform to the topological scenario.[7–9] In spite of this progress, today—nearly a decade since the original publication—it is still debated whether the proposal by Dzero et al. applies to SmB$_6$ which consequently would make it the first strongly correlated topological insulator at all. Various experimental methods have led to contradicting conclusions. In particular, the disagreement about crystal termination between scanning tunneling microscopy (STM) and angle-resolved photoemission (ARPES) studies has been emphasized as major hindrance toward a solution of this fundamental controversy.[4] A variety of surface terminations has been suggested on the basis of STM: A (2 × 1) structure was interpreted as a missing-row reconstruction,[10,11] because bulk truncated (100) surfaces are polar and

H. Herrmann, Prof. M. Sterrer
Institut für Physik
Karl-Franzens-Universität Graz
Universitätsplatz 5, 8010 Graz, Austria

Dr. P. Hlawenka, Dr. K. Siemensmeyer, Dr. E. Weschke,
Dr. J. Sánchez-Barriga, Dr. A. Varykhalov, Prof. O. Rader, Dr. E. D. L. Rienks
Helmholtz-Zentrum Berlin für Materialien und Energie
Elektronenspeicherring BESSY II
Albert-Einstein-Straße 15, 12489 Berlin, Germany
E-mail: emile.rienks@helmholtz-berlin.de

The ORCID identification number(s) for the author(s) of this article can be found under https://doi.org/10.1002/adma.201906725.

Dr. N. Y. Shitsevalova, Dr. A. V. Dukhnenko, Dr. V. B. Filipov
Institute for Problems of Materials Science
National Academy of Sciences of Ukraine
Krzhyzhanovsky str. 3, 03142 Kiev, Ukraine

Dr. S. Gabáni, Dr. K. Flachbart
Institute of Experimental Physics
Slovak Academy of Sciences
Watsonova 47, 04001 Košice, Slovakia

Dr. E. D. L. Rienks
Institut für Festkörperphysik
Technische Universität Dresden
01062 Dresden, Germany

Dr. E. D. L. Rienks
Leibniz-Institut für Festkörper- und Werkstoffforschung Dresden
Helmholtzstraße 20, 01069 Dresden, Germany

**ADVANCED
SCIENCE NEWS**

www.advancedsciencenews.com

**ADVANCED
MATERIALS**

www.advmat.de

the reconstruction would lift the polarity. Areas with (1 × 1) structure have nonetheless been reported as well.[10–12] Rößler et al. have interpreted some (1 × 1) areas as B and some as Sm terminated.[11] Seemingly different (1 × 1) topographies are also reported by Sun et al.[13] Finally, apparently unstructured areas were found to be abundant,[10,12] with areas of the well-ordered topographies (2 × 1) and (1 × 1) existing only on small length scales.[10] ARPES results, on the other hand, strongly suggest the existence of just two distinct, chemically pure terminations.[14] Because the ARPES method averages over macroscopic areas, this result means that the single dominant termination persists on the scale of hundreds of micrometers.[15]

Here, we resolve this apparent contradiction by studying surfaces prepared from the same crystal with STM and ARPES. Scanning tunneling spectroscopy (STS) further probes the local density of states (LDOS) and can be used to test a hypothesis based on ARPES results, namely that surface shifts of the 4f-like states at E_F cause the surface conductivity in SmB_6.[14] The results of our comparative study allow us to link the ordered STM topographies reported earlier,[10,11] to the two crystal terminations seen in photoemission.[14,15] We show that our STM and ARPES results, which are consistent with earlier studies, can be understood in the same manner: Tiny energy shifts of the order of +10 and −10 meV are present on the two crystal terminations and these surface shifts are the trivial explanation for the surface states measured in nearly all ARPES studies on SmB_6.

STM and ARPES experiments were done using surfaces prepared from the same floating zone grown SmB_6 crystal.[14] STM experiments were performed at a temperature of 6 K on samples cleaved in ultrahigh vacuum at $T = 80$ K. The latter is higher than the temperatures $T \leq 30$ K at which samples have been cleaved in earlier studies.[10,11] The obtained surface structures appear nonetheless very similar, although exposure of the relatively warm surface to the residual gas may have led to a larger number of defects. In order to obtain a maximum signal at the required energy resolution, a 5 mV peak-to-peak bias modulation amplitude is used in STS.

Photoemission measurements were done using the 1³-ARPES experiment at BESSY II's UE112-PGM2b beamline. Samples are cleaved in ultrahigh vacuum at temperatures below 45 K. Spatial resolution is determined by the size of the synchrotron beam with a full width at half maximum (FWHM) of ≈250 μm, the energy resolution is 3 meV.

We have studied surfaces prepared by cleaving pieces cut from the same ingot with both ARPES and STM in order to find a relationship between the results from both methods. From photoemission we obtain the following properties: The first striking result is that surfaces prepared from this crystal tend to consist of areas exceeding the size of the synchrotron light spot, in which a single termination dominates the photoemission signal. In **Figure 1** we show a set of measurements from ten independently prepared surfaces. The results on the left and right of panel (a) clearly form two distinct sets, even though they are obtained under identical conditions. The results in the left column of Figure 1a can be associated with B termination on the basis of the corresponding B 2p and Sm 4f spectra, those on the right with Sm termination.[14]

The energy distribution curves in Figure 1b show that the Sm 4f-like intensity at $k_{||} = (3\pi/4a, 0)$ is displaced for the two

different terminations by an amount that is roughly equivalent to the peak width. We can therefore conclude that the distribution of the results is bimodal with negligible overlap between the modes: The energy distribution curves from B terminated samples (blue) have less than 20% of their maximum intensity at $E_B = 10$ meV (indicated by the dashed vertical line in Figure 1b). Spectra from Sm terminated samples (red), on the other hand, have attained >85% of their maximum intensity at this binding energy.

In Figure 1c we present the photoemission intensity integrated along the $\overline{\Gamma}–\overline{X}$ direction, in order to see to what extent the angle-integrated LDOS will differ for the two terminations. The maxima of the curves in Figure 1c are displaced by ≈5 meV (Δ_{LDOS}). We can thus expect that part of the surface shifts observed in ARPES will persist in tunneling spectra obtained on differently terminated surfaces. The dashed vertical lines in Figure 1c indicate the normal emission energies of the surface component on the B (blue) and Sm terminated surface (red) along with the position of the more bulk-like 4f component common to both terminations.

The data in Figure 1 represent about half of the surfaces prepared from this crystal that we have studied with ARPES. Figure 1 features results from the subset on which we have performed the experiment under the same conditions: $h\nu = 31$ eV, s-polarization, $\overline{\Gamma}–\overline{X}$ orientation. We find a large majority (≈90%) of all surfaces to have single termination areas that exceed the size of the synchrotron light spot, which means they are larger than ≈7×10^5 μm². In fact, with a sample size of ≈1 mm² we typically find a single termination to dominate the entire sample surface.

We can now draw the following conclusions from the photoemission experiments that will prove important for the interpretation of the STM results:

1. The crystal tends to expose areas on the mm-scale that are dominated by a single termination.
2. By combining valence and B 2p core-level spectra we can conclude that either termination appears to have only a single undercoordinated element, i.e., is purely Sm or B terminated.[14]
3. Finally, we find both terminations to show umklapp features in ARPES indicative of superstructures with twice the lattice constant. This result is presented in Figure S1 in the Supporting Information.

With STM we have encountered two distinct topographies on different surfaces prepared from pieces of the same crystal used in the photoemission experiments above:

- (2 × 1) reconstructed areas with a prominent maximum near −7 mV in tunneling spectra, shown in **Figure 2**a,b.
- Seemingly unreconstructed areas with a less structured low-bias spectrum, given in Figure 2c,d.

Both Yee et al. and Rößler et al. have observed well-ordered surface areas with very similar characteristics:[10,11] A (2 × 1) topography with dI/dV spectra nearly identical to that shown in Figure 2b has been reported by both groups. Both Yee et al. and Rößler et al. have also observed well-ordered (1 × 1) topographies, but spectra from these areas show a larger variation: Rößler et al. have reported two kinds of spectra from (1 × 1)
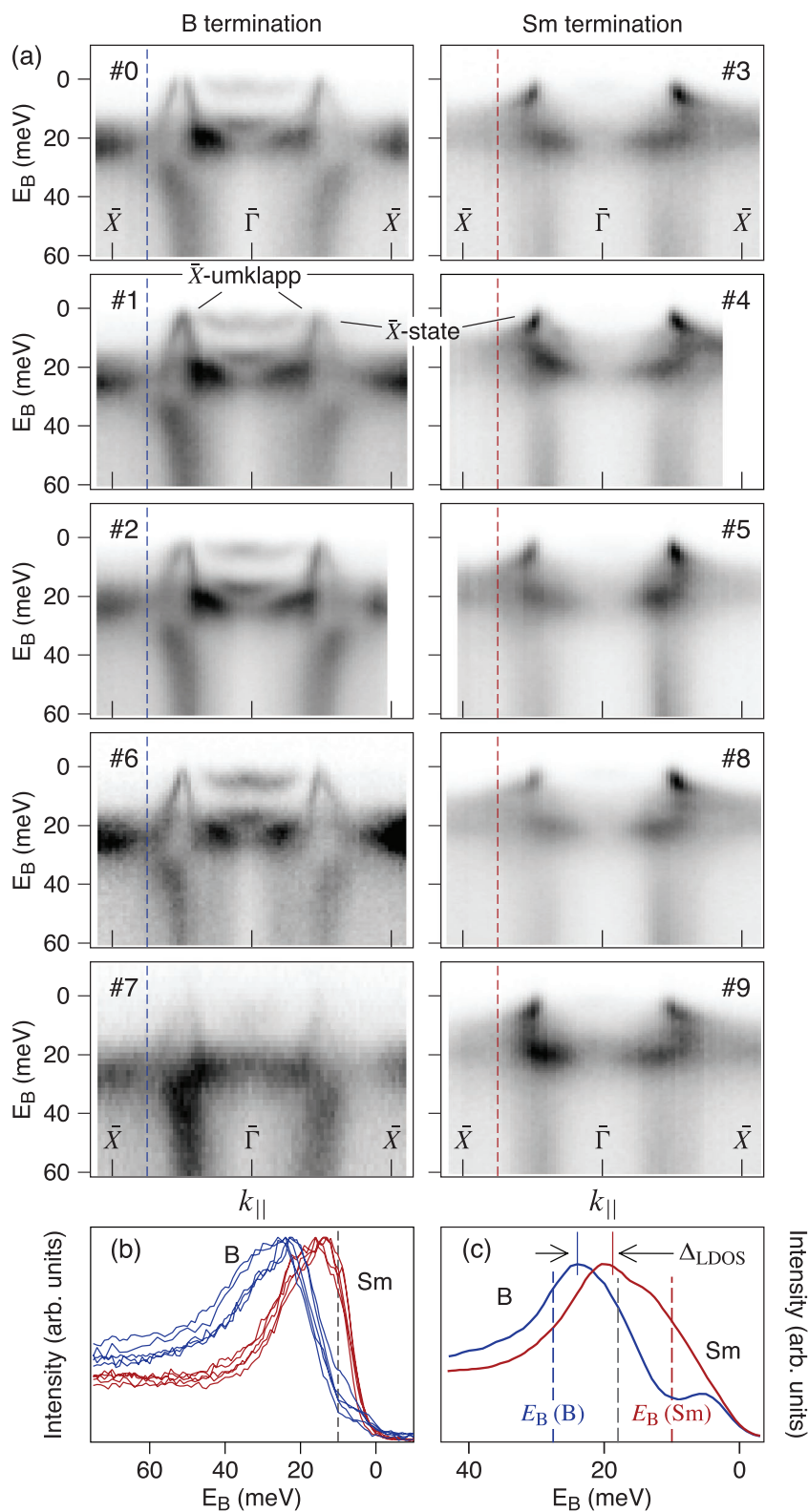
Figure 1. The two terminations in ARPES. a) Photoemission intensity from ten independently prepared surfaces obtained under identical conditions ($h\nu = 31$ eV; s-polarization). The results in the left (right) column are assigned to B termination (Sm termination). The label (#) indicates the order in which the surfaces were prepared. b) Energy distribution curves at $k_{||} = -3\pi/4a$ [dashed vertical lines in (a)]. c) Angle-integrated photoemission intensity from #6 (blue) and #8 (red). The difference between maxima (Δ_{LDOS}) amounts to 5 meV. Dashed lines in (c) indicate the position of surface components at $\bar{\Gamma}$ for B [E_B (B)] and Sm termination [E_B (Sm)] identified by Hlawenka et al.[14]

topographies. One type is very similar to that in Figure 2d, i.e., Fano resonance-like with $q \approx 0$, while the second one has a more pronounced maximum at the negative bias side.[11] Yee et al. report only one type of tunneling spectra.[10] These are more similar to the second one with a prominent maximum near −28 mV on the (1 × 1) areas.[10] In two sub-Kelvin studies Jiao et al.[17] and Sun et al.[13] observe on (1 × 1) areas nearly identical fine structure spectra.

An important departure from earlier publications is that we only find a single type of topography on a given surface. In contrast, Rößler et al. report that (1 × 1) regions form a rare exception to (2 × 1) areas,[11] while Yee et al. even find the majority of the surface to be disordered.[10] We attribute our result to the presence of large single-termination areas (photoemission result 1). Given that the illuminated area in ARPES is more than six orders of magnitude larger than the STM scan range, it is not feasible to confirm directly that a single topography has the same extent. Instead, we have sampled the cleaved area in different locations separated by hundreds of micrometers. The probability of finding only one out of two equally abundant topographies decreases rapidly with an increasing number N of independent samplings ($p = 2^{-N} < 1\%$ for $N > 6$). We have approached each cleaved surface with the tip in a sufficient number of different locations to render this probability negligible. We therefore propose that the distinct topographies presented in Figure 2 correspond to the photoemission terminations.

We propose an assignment, i.e., which topography corresponds to which termination, based on the following result: We find the STM contrast on the (1 × 1) topography to depend strongly on the bias voltage. This is illustrated in **Figure 3** where the corrugation maxima shift by half a lattice constant depending on the bias voltage. We attribute this effect to a different energy dependence for the density of Sm and B-derived states. Bulk band structure calculations[18,19] reveal a several eV wide gap in the B 2p density of states around E_F. The validity of this view at the surface is reinforced by the results of Denlinger et al. who have successfully
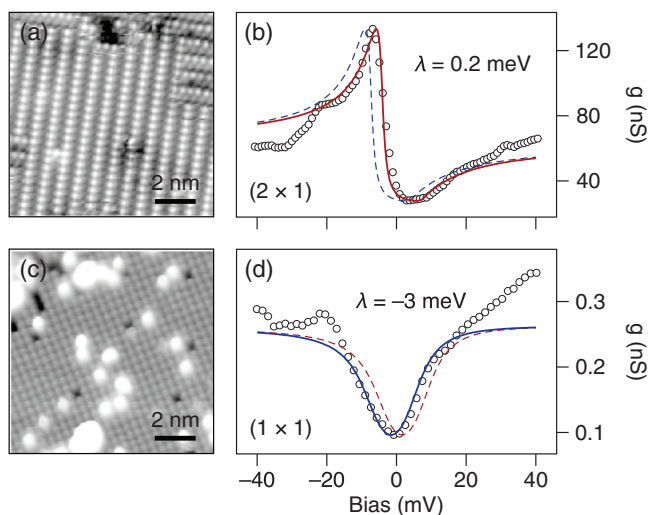
**ADVANCED
SCIENCE NEWS**

www.advancedsciencenews.com

**ADVANCED
MATERIALS**

www.advmat.de

Figure 2. The two terminations in STM and STS. a) (2×1) reconstructed topography ($V_b = -9$ mV, $I_{set} = 4.1$ nA) with corresponding b) experimental tunneling spectrum (markers) along with model description (solid line). c) (1×1) topography ($V_b = -3$ V, $I_{set} = 840$ pA) with d) corresponding tunneling spectrum. We assign the (2×1) structure to Sm termination and the (1×1) to B, see text. The dashed lines in (b) and (d) show model descriptions with λ values optimized for the other topography, see text.

matched the occupied part of the calculated B 2p band structure to photoemission results.[15] We treat this topic in more detail in Figures S2 and S3 in the Supporting Information. Since SmB_6 has the CsCl crystal structure, the corrugation maximum can shift from Sm to B_6 sites depending on which states dominate the tunnel current.

The $a/2$ phase shift of the corrugation is only seen on the (1×1) surface. Using the photoemission result 2 that the terminations are chemically pure, we can conclude that the (1×1) topography corresponds to B termination: With the B 2p states spatially closer to the tip, the B contribution will start to dominate the tunneling current at bias voltages above the B 2p density of states threshold ($|V_b| \leq 1$ V). At the Sm terminated surface, on the other hand, the outermost Sm layer is closer to the tip and therefore likely to dominate over the entire bias voltage range. We can thus assign the (1×1) topography shown in
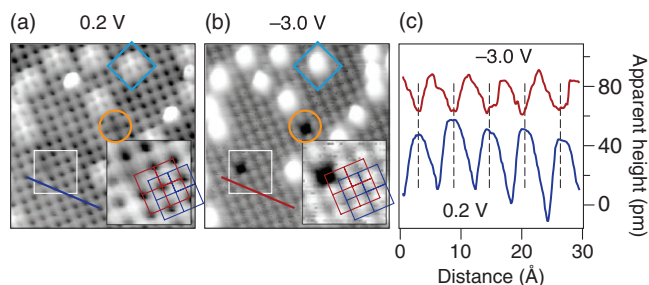

Figure 3. Demonstration of contrast inversion. a,b) STM topographs with bias voltages of 0.2 V (a) and −3.0 V (b); current: $I_{set} = 86$ pA and $I_{set} = 260$ pA, respectively. The insets in (a) and (b) highlight the area indicated by the white squares. Circles (orange) and diamonds (blue) in (a) and (b) highlight the two most common types of defect on this topography. c) Line profiles indicated by blue and red lines in (a) and (b). Dashed lines separated by $a\sqrt{2}$ indicate a contrast inversion.

Figure 2c to B termination. Another consequence of the energy dependence of the B density of states is that an absolute bias voltage larger than ≈1 V is required to access B 2p states and reliably image the location of B atoms.

The circles and diamonds in Figure 3a,b highlight the two most common defects we find on the (1×1) surface. The circled defect appears as a weak depression at low bias but becomes much more prominent at $V_b = -3$ V. Using the reasoning that led to the above assignment we conclude that this type corresponds to a defect in the surface B layer. The other type of defect highlighted with the diamond is relatively pronounced at both bias voltages. It appears at on-top sites of the low-bias lattice (and consequently in the hollow site of the high-bias, presumably B lattice).

Since STS also provides experimental access to the density of states, we can try and establish further connections. Hlawenka et al. have observed termination-dependent shifts of the 4f-like intensity near E_F using photoemission:[14] A 4f component appears at a binding energy $E_B \approx 28$ meV, about 10 meV below the bulk peak for B termination. Interestingly, both Yee et al.[10] and Rößler et al.[11] have reported a feature near this energy (−27 and −28 mV) in tunneling spectra obtained on the (1×1) topography. This result supports the interpretation given above that the (1×1) topography corresponds to the B terminated surface. In addition, the prominent feature near −7 mV in tunneling spectra on the (2×1) topography nearly coincides with a surface component seen in photoemission for the Sm terminated surface ($E_B \approx 9$ meV, i.e., about 10 meV above the bulk component[14]). Jiao et al. and Sun et al. further reported a fine structure in sub-Kelvin tunneling spectra.[13,17] It is tempting to interpret this fine structure in terms of peaks in the LDOS, and the attribution to crystal electric field splitting seems reasonable.

Interference between parallel tunneling pathways, however, complicates the differential conductance spectra in Kondo systems.[16,20] We interpret the spectra using a model for tunneling into a Kondo lattice by Maltseva et al.,[16] more detail is provided in the Supporting Information.

The most relevant model parameter in the present context is the energy λ at which the structure in the differential conductance is observed. Since λ relates directly to the energy of the renormalized 4f level, i.e., the energy of the Kondo resonance, we should expect it to reflect the different surface 4f binding energies seen in ARPES. We indeed find that agreement between model and data can only be obtained by assuming a different value of λ for the different topographies in Figure 2b,d. We find that $\lambda = 0.2$ meV matches the experimental spectrum on the (2×1) surface, while −3 meV fits the (1×1) case. This shift of the renormalized 4f energy further supports the assignment of the (2×1) reconstructed topography to Sm termination, and the (1×1) to B termination: With ARPES the smaller surface 4f binding energy is found at the Sm terminated surface. In addition, the difference between λ values of 3.2 meV matches the estimated difference between LDOS maxima for B and Sm termination of 5 meV (Δ_{LDOS} in Figure 1c) rather closely.

Before concluding, we will discuss the assignment we propose with respect to the literature. Where we propose that the unreconstructed topography corresponds to the B terminated

surface, Rößler et al. have assigned (1×1) areas with a slightly different appearance to B and Sm termination.[11] We question this assignment, because it is based on results with bias voltages where B states are not expected to contribute noticeably to the tunnel current. In addition, as the spectra obtained on these areas appear indistinguishable, we suggest that they should all be attributed to B termination.

Both Yee et al.[10] and Rößler et al.[11] assign the (2×1) structure to a Sm missing-row reconstruction. While such a structure would avert divergence of the electrostatic surface potential at the bulk-truncated (100) surface, we note that a missing-row structure is not compatible with result 2 from our photoemission experiments: There appears to be no distinct termination with both undercoordinated B and Sm atoms.[14] Whatever the nature (structural or electronic) of the of the (2×1) superstructure, we expect that it only consists of undercoordinated Sm atoms.

Back-folded photoemission intensity, reported in several ARPES studies,[7,8,14] could provide a further test for the assignment of STM topographies to terminations, but as we demonstrate in Figure S1 of the Supporting Information, the photoemission results from both terminations bear signs of a $2a$ superstructure. Since only one of the STM topographies shows a clear superstructure we cannot use this result to correlate terminations and topographies. Using our assignment of the (2×1) topography to Sm termination and the (1×1) topography to B termination, the origin of the umklapp intensity is accounted for at the former, but remains a question for the latter termination. We propose the superstructure observed in ARPES for B termination could be due to a subtle effect such as a tilt of the B octahedra, not easily seen in STM.

In conclusion, we present a consistent view of the SmB_6 (100) surface by combining STM and ARPES experiments on surfaces of the same crystal. Using the element-specific state densities, we conclude that the (1×1) STM topography corresponds to B termination, and the (2×1) to Sm termination. We find the differential conductance of the different topographies to be distinct, and show that this result supports the interpretation that a shift of the Sm 4f-like state is the trivial origin of the SmB_6 surface states.

Supporting Information

Supporting Information is available from the Wiley Online Library or from the author.

Acknowledgements

Conflict of Interest

The authors declare no conflict of interest.

Keywords

[1] M. Dzero, V. Galitski, *J. Exp. Theor. Phys.* **2013**, *117*, 499.
[2] D. Pesin, L. Balents, *Nat. Phys.* **2010**, *6*, 376.
[3] M. Dzero, K. Sun, V. Galitski, P. Coleman, *Phys. Rev. Lett.* **2010**, *104*, 106408.
[4] J. W. Allen, *Philos. Mag.* **2016**, *96*, 3227.
[5] S. Wolgast, Ç. Kurdak, K. Sun, J. W. Allen, D.-J. Kim, Z. Fisk, *Phys. Rev. B* **2013**, *88*, 180405.
[6] D.-J. Kim, S. Thomas, T. Grant, J. Botimer, Z. Fisk, J. Xia, *Sci. Rep.* **2013**, *3*, 3150.
[7] N. Xu, X. Shi, P. K. Biswas, C. E. Matt, R. S. Dhaka, Y. K. Huang, N. C. Plumb, M. Radović, J. H. Dil, E. Pomjakushina, K. Conder, A. Amato, Z. Salman, D. M. Paul, J. Mesot, H. Ding, M. Shi, *Phys. Rev. B* **2013**, *88*, 121102.
[8] J. Jiang, S. Li, T. Zhang, Z. Sun, F. Chen, Z. R. Ye, M. Xu, Q. Q. Ge, S. Y. Tan, X. H. Niu, M. Xia, B. P. Xie, Y. F. Li, X. H. Chen, H. H. Wen, D. L. Feng, *Nat. Commun.* **2013**, *4*, 3010.
[9] G. Li, Z. Xiang, F. Yu, T. Asaba, B. Lawson, P. Cai, C. Tinsman, A. Berkley, S. Wolgast, Y. S. Eo, D.-J. Kim, Ç. Kurdak, J. W. Allen, K. Sun, X. H. Chen, Y. Y. Wang, Z. Fisk, L. Li, *Science* **2014**, *346*, 1208.
[10] M. M. Yee, Y. He, A. Soumyanarayanan, D.-J. Kim, Z. Fisk, J. E. Hoffman, *arXiv:1308.1085*, **2013**.
[11] S. Rößler, T. H. Jang, D.-J. Kim, L. H. Tjeng, Z. Fisk, F. Steglich, S. Wirth, *Proc. Natl. Acad. Sci. USA* **2014**, *111*, 4798.
[12] W. Ruan, C. Ye, M. Guo, F. Chen, X. Chen, G.-M. Zhang, Y. Wang, *Phys. Rev. Lett.* **2014**, *112*, 136401.
[13] Z. Sun, A. Maldonado, W. S. Paz, D. S. Inosov, A. P. Schnyder, J. J. Palacios, N. Y. Shitsevalova, V. B. Filipov, P. Wahl, *Phys. Rev. B* **2018**, *97*, 235107.
[14] P. Hlawenka, K. Siemensmeyer, E. Weschke, A. Varykhalov, J. Sánchez-Barriga, N. Y. Shitsevalova, A. V. Dukhnenko, V. B. Filipov, S. Gabáni, K. Flachbart, O. Rader, E. D. L. Rienks, *Nat. Commun.* **2018**, *9*, 517.
[15] J. D. Denlinger, J. W. Allen, J.-S. Kang, K. Sun, B.-I. Min, D.-J. Kim, Z. Fisk, *JPS Conf. Proc.* **2014**, *3*, 017038.
[16] M. Maltseva, M. Dzero, P. Coleman, *Phys. Rev. Lett.* **2009**, *103*, 206402.
[17] L. Jiao, S. Rößler, D.-J. Kim, L. H. Tjeng, Z. Fisk, F. Steglich, S. Wirth, *Nat. Commun.* **2016**, *7*, 13762.
[18] V. Antonov, B. Harmon, A. Yaresko, *Phys. Rev. B* **2002**, *66*, 165209.
[19] F. Lu, J. Zhao, H. Weng, Z. Fang, X. Dai, *Phys. Rev. Lett.* **2013**, *110*, 096401.
[20] J. Figgins, D. K. Morr, *Phys. Rev. Lett.* **2010**, *104*, 187202.